Electronic Supplementary Material (ESI) for Catalysis Science & Technology.


# Supporting Information

# Nitrogen-doped carbon nanotubes as efficient catalysts for isobutane dehydrogenation

Jiali Mu,[a] Liam John France,[a] Baoan Liu,[a] Junjun Shi,[a] Jinxing Long,[a] LuFeng Lv,*[b] Xuehui Li*[a]

[a] School of Chemistry and Chemical Engineering, Pulp & Paper Engineering State Key Laboratory of China, South China University of Technology, Guangzhou 510640, PR China.
Email: cexhli@scut.edu.cn

[b] Sinopec Research Institute of Petroleum Processing, Beijing 100083, PR China
Email: lvlf.ripp@sinopec.com

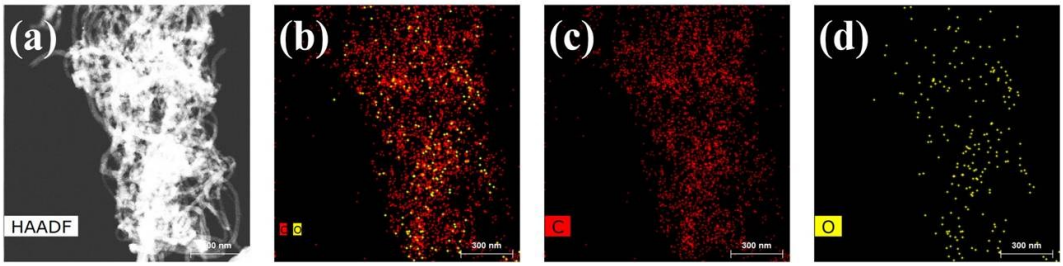


Fig. S1 Scanning transmission electron microscopy (STEM) elemental mapping of oMWCNTs: a) High angle annular dark-field (HAADF) showing the mapping area, b) overlay map of C and O, and c-d) elemental mapping for C and O elements respectively.

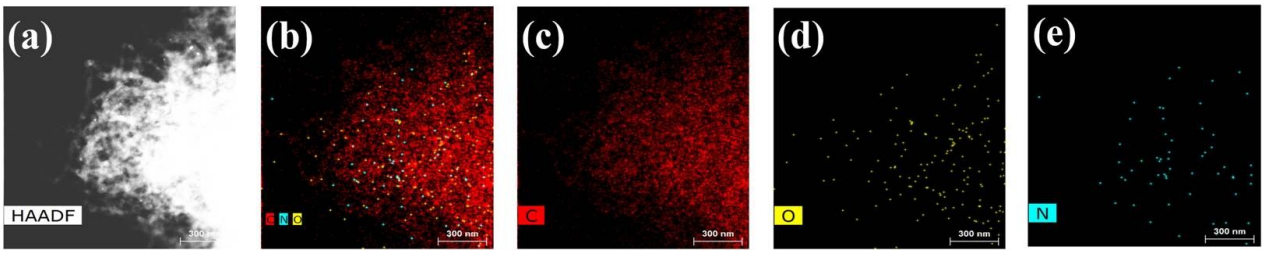


Fig. S2 Scanning transmission electron microscopy (STEM) elemental mapping of $N_{13}$-oMWCNTs: a) High angle annular dark-field (HAADF) showing the mapping area, b) overlay map of C, O and N, and c-e) elemental mapping for C, O and N elements, respectively.

Table S1 Textural properties of the catalysts.

| Samples | BET surface area ($m^2\ g^{-1}$) | Pore volume ($cm^3\ g^{-1}$) |
|---|---|---|
| pristine MWCNTs | 134 | 0.55 |
| oMWCNTs | 157 | 0.74 |
| $N_5$-oMWCNTs | 185 | 0.94 |
| $N_{10}$-oMWCNTs | 181 | 0.83 |
| $N_{13}$-oMWCNTs | 185 | 0.82 |
| $N_{15}$-oMWCNTs | 175 | 0.82 |
| $N_{20}$-oMWCNTs | 178 | 0.92 |

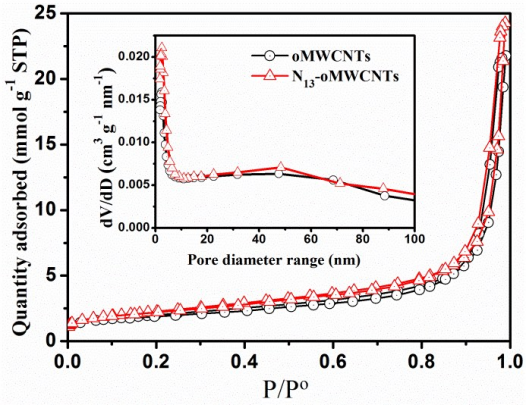


Fig. S3 Nitrogen adsorption-desorption isotherms and pore size distribution of oMWCNTs and $N_{13}$-oMWCNTs.

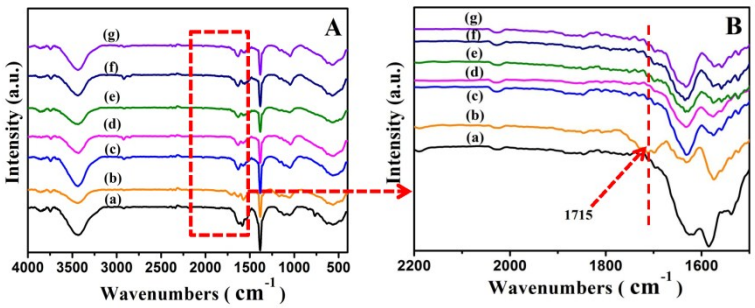


Fig. S4 (A) FTIR spectra – 400-4000 cm$^{-1}$ (B) FTIR spectra – 1500-2200 cm$^{-1}$ of (a) pristine MWCNTs, (b) oMWCNTs, (c)-(f) $N_x$-MWCNTs catalysts (where x represent 5, 10, 13, 15, 20).

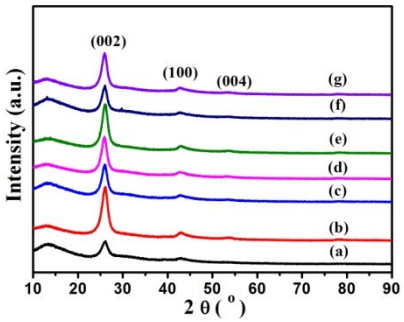


Fig. S5 XRD patterns of (a) pristine MWCNTs, (b) oMWCNTs, (c)-(f) $N_x$-MWCNTs catalysts (where x represent 5, 10, 13, 15, 20).

Table S2 Textural properties of catalysts after 12 h reaction.

| Samples | BET surface area ($m^2$ $g^{-1}$) | Pore volume ($cm^3$ $g^{-1}$) |
|---|---|---|
| oMWCNTs | 127 | 0.87 |
| $N_5$-oMWCNTs | 132 | 0.83 |
| $N_{13}$-oMWCNTs | 104 | 0.90 |
| $N_{20}$-oMWCNTs | 128 | 0.80 |

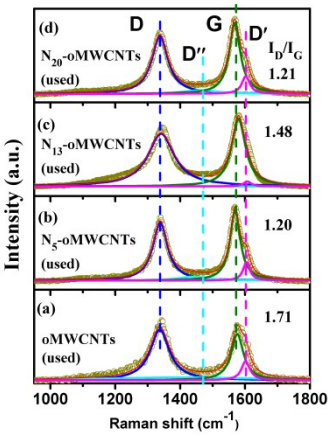


Fig. S6 Deconvoluted Raman spectra of (a) oMWCNTs and (b)-(d) $N_x$-oMWCNTs catalysts (x represent 5-20) after 12 h reaction.

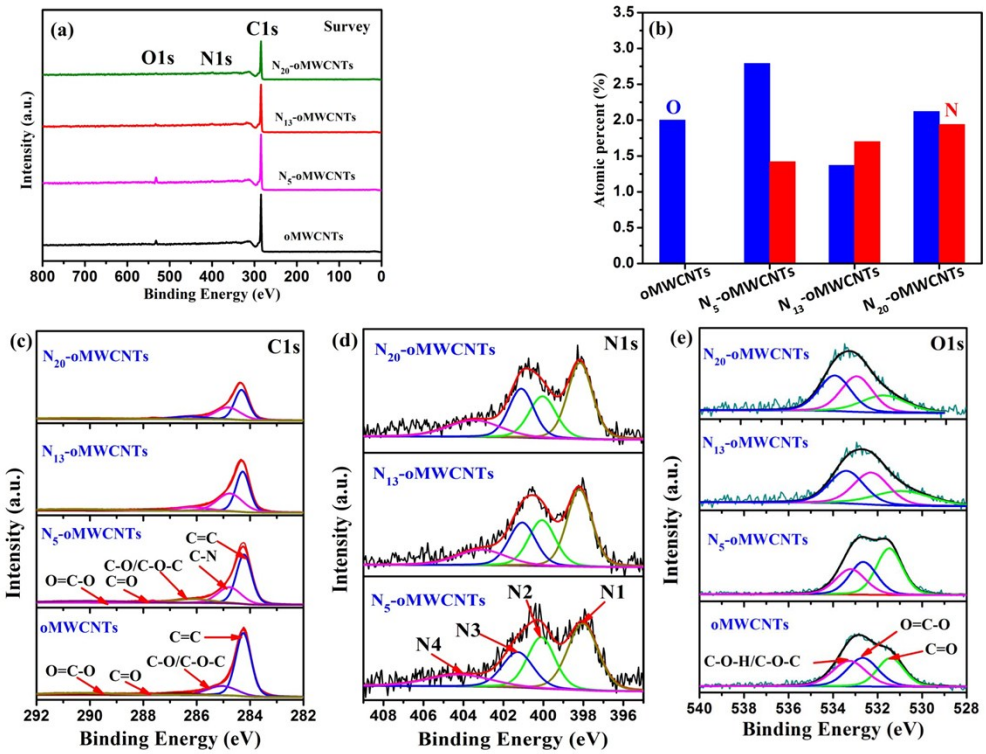


Fig. S7 (a) XPS survey spectra of different catalysts after 12 h reaction. (b) Atomic percentage of oxygen (blue) and nitrogen (red). High-resolution (c) C1s, (d) N1s and (e) O1s spectra.

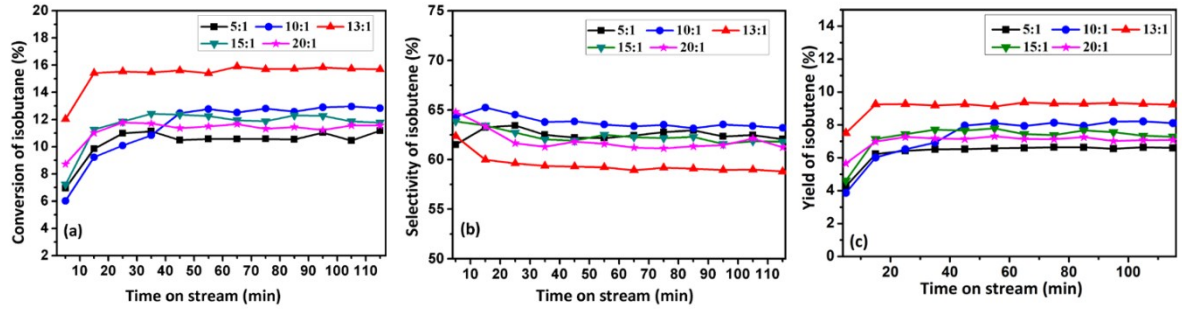


Fig. S8 Catalytic performance of the as-synthesized oMWCNTs and $N_x$-oMWNCTs catalysts for the DDH reaction. Reaction conditions: T=600 °C, GHSV = 3.0 L $g^{-1}$ $h^{-1}$. $V_{i\text{-}C4H10}$ / $V_{N2}$ =1:1.

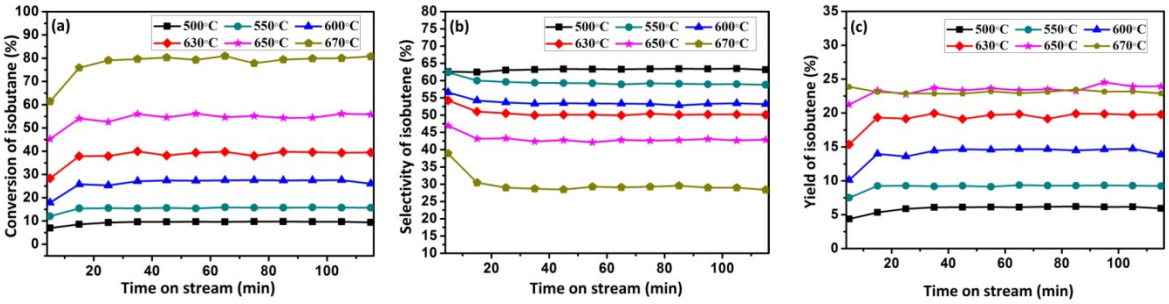


Fig. S9 The influence of reaction temperature on the activity of $N_{13}$-oMWCNTs catalyzed DDH reaction. Reaction conditions: $V_{i\text{-}C4H10}$ / $V_{N2}$ =1:1, GHSV = 3.0 L $g^{-1}$ $h^{-1}$.

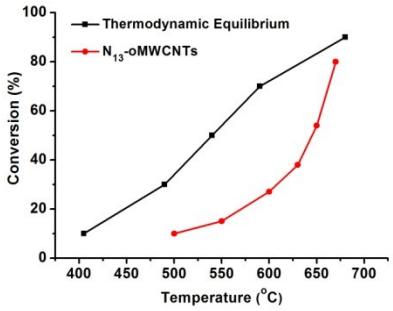


Fig. S10 Thermodynamic equilibrium conversion according to reference[1] (black) and experimentally determined conversion of $N_{13}$-oMWCNTs at different temperature (red).
Reaction conditions: $V_{i\text{-}C4H10}$ / $V_{N2}$ =1:1, GHSV = 3.0 L $g^{-1}$ $h^{-1}$.

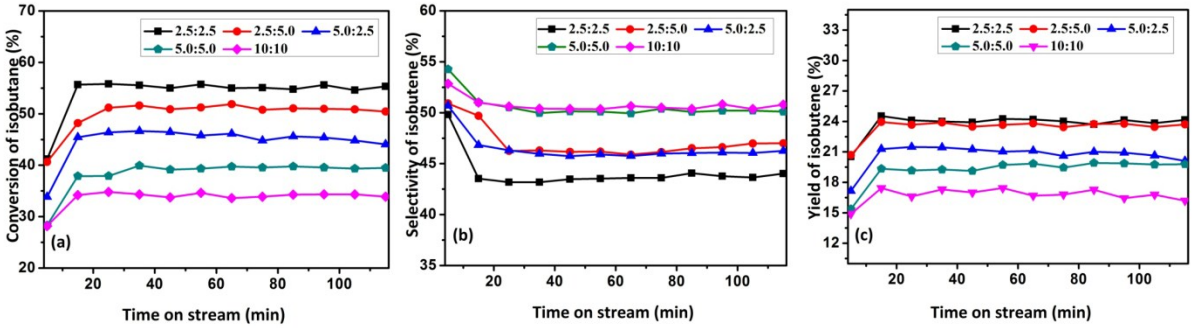


Fig. S11 The influence of gas flow rate on the activity of $N_{13}$-oMWCNTs catalyzed DDH reaction.
Reaction conditions: T=630 °C, $V_{i\text{-}C4H10}$ : $V_{N2}$= 2.5:2.5~10:10 mL $min^{-1}$.

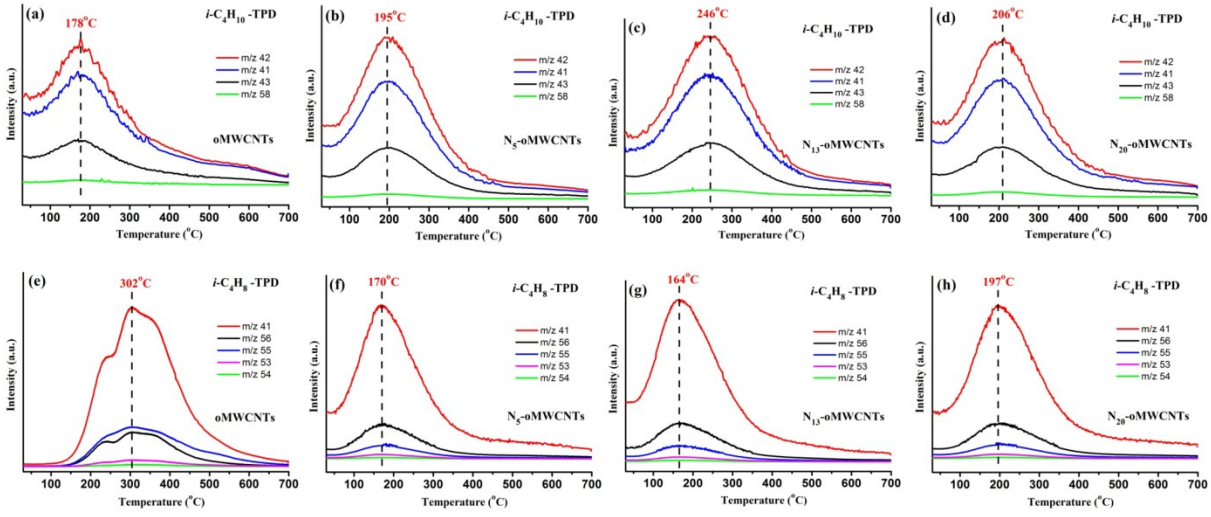


Fig. S12 $i$-$C_4H_{10}$ and $i$-$C_4H_8$ TPD profiles of oMWCNTs and $N_x$-oMWCNTs catalysts before reaction.

Refrences

1 B. M. Wechhuysen and R. A. Schoonheydt, *Catal. Today*, 1999, 51, 223-232.